Thermal characterization of building walls under random boundary conditions

Emilio Sassine, Yassine Cherif, Emmanuel Antczak, Joseph Dgheim

Thermal identification of building walls under random boundary conditions

Emilio SASSINE[1,*]; Yassine CHERIF[2,*]; Emmanuel ANTCZAK[2]; Joseph DGHEIM[1]

[1] Lebanese University, Habitat and Energy Unit, Group of Thermal and Renewable Energies - Laboratory of Applied Physics (LPA-GMTER), Faculty of Sciences, Fanar Campus, Lebanon

[2] University of Artois, Laboratory of Civil Engineering and Geo-Environment (LGCGE - EA 4515) Technoparc Futura, F-62400 Béthune, France

Abstract

This work aims to improve the knowledge on dynamic thermophysical characterization of building envelopes by comparing three numerical methods applied on an experimental wall made of masonry brick. The thermal conductivity λ and the thermal capacity ρc_p are determined by performing identification between the experimental measurements of the heat flux and the heat flux resulting from these numerical models. The experimental device consists of a thermal box with a controlled ambiance through a radiator linked to a thermostatic bath and placed inside the thermal box, on the opposite side facing the wall. Three different methods were examined: The Heat Transfer Matrix analytical method (HTM) using the heat transfer matrix, the Finite Element Method (FEM) using COMSOL Multiphysics® software, and the Building Simulation Model method (BSM) using TRNSYS® Type 56 coupled with Genopt® optimization tool. The reproducibility of the methods was also validated through two other datasets (one random and one harmonic). The obtained results were satisfactory for both λ and for ρc_p and for the three studied methods with deviations less than 5% between the results of the different methods. The data logging duration for random boundary conditions was found to be around five days while in harmonic boundary conditions two days were sufficient for the solution to converge.

[*] *Corresponding authors :*
Emilio SASSINE, Email address: emilio.sassine@gmail.com, Habitat and Energy Unit, Laboratory of Applied Physics (LPA), Lebanese University, Faculty of Sciences, Fanar Campus, Lebanon.

Yassine CHERIF, Email address: yassine.cherif@univ-artois.fr, University of Artois, Laboratory of Civil Engineering and Geo-Environment (LGCgE - EA 4515) Technoparc Futura, F-62400 Béthune, France.

NOMENCLATURE

Symbols	
C	Surface equivalent thermal capacity ($J.m^{-2}.K^{-1}$)
c_p	Specific heat ($J.kg^{-1}.K^{-1}$)
e	Material thickness (m)
p	Laplace transform variable (-)
R	Thermal resistance ($m^2.K\ W^{-1}$)
T	Temperature (°C)
t	Time (s)
Greek letters	
λ	Thermal conductivity ($W.m^{-1}K^{-1}$)
φ	Heat flux ($W\ m^{-2}$)
ρ	Density ($kg.m^{-3}$)
Indexes	
amb	Ambient
i	Interior surface
o	Exterior surface
w	Wall
exp	Experimental measured value
num	Numerical simulated value

Keywords

Building components; heat transfer; thermal characterization; random temperature profile; dynamic thermal simulation

1 Introduction

Thermal improvement of building envelopes is gaining more attention by the scientific community due to the ever growing energy and environmental issues related greenhouse gases emissions and fossil fuels limitations as well as the increase of the living standards and thermal comfort. In order to predict the energy demand of new or existing buildings, some building attributes need to be determined and most importantly the thermophysical properties of building elements [1].

There are many non-destructive testing methods used for determining physical parameters based on data logging during a certain time range varying between few minutes to several months depending on the application. Many steady-state thermal modeling approaches [2] based on static thermal parameters such as thermal conductivities, thermal resistances, or thermal transmittances *U*, are still used in many studies. The thermo-fluxmetric [3, 4] method is used to determine the static thermal properties of building elements in the laboratory steady-state conditions.

Nevertheless, in real situations, external boundary conditions are always dynamic from both sides of building elements. From the outside, the wall is subjected to outdoor dynamic conditions such as solar radiation, temperature, and wind; and from the inside, some internal factors such as use of heating or air-conditioning systems and occupants' behavior.

Several works deal with the thermal characterization of building elements under dynamic boundary conditions. Among the few research works addressing the thermal characterization of transparent building elements, Cornaro et al. [5] proposed an in-situ method to evaluate the thermal performance of transparent building elements. The results were satisfactory for estimating the Solar Heat Gain Coefficient (SHGC), however, the determination of the Global thermal transmittance was not accurate due to the very small inner and outer surface temperature.

A simple thermal characterization method provided by the ISO 9869 [6] and based on in-situ measurements using only two thermocouples and a heat flux sensor allow the determination of the walls' thermal resistance. Rasooli et al. [7] proposed some improvements for this method by suggesting an additional heat flux sensor to reduce the data logging duration and improve the accuracy.

Berger et al. [8] used the Bayesian inference statistical method for estimating the thermal conductivities and the convective heat coefficient of an old historical building wall. The results were promising, but they don't allow the determination of the dynamic thermal properties, which were defined from the literature. On the other hand, Gori et al. [9] succeeded in determining the dynamic thermal properties for two thick walls: a solid brick wall and a multilayered wall (aerated clay, plaster, fiberglass insulation and plasterboard) using the Bayesian inference method. Two thermal mass models (1TM and 2TM) were identified for each wall and the method provided satisfactory results; however, the reproducibility of the results was not verified by using more than one dataset for each wall.

The EN ISO 13786 [10] standard provides methods for the calculation of dynamic thermal characteristics of building components.

Baldinelli et al. [12] used the EN ISO 13786 standard for determining the amplitude and the time lag in laboratory conditions with one-day period sinusoidal solicitations using a thermal chamber. However, the method lacks of precision and is limited to harmonic boundary conditions, making it unsuitable for in situ measurements.

Ricciu et al. [13] also used the same approach with harmonic solicitations for determining the thermal properties (the specific heat and thermal conductivity of the layers of an experimented wall using a climatic chamber and obtained quite different results between the properties declared by the manufacturer and the measured ones (even more than three time greater).

Even though the harmonic solicitations provide accurate results for dynamic thermal properties, they are only valid for laboratory conditions and could not be used for existing building walls. The harmonic solicitations were adopted by Petojević et al. [11] to determine the dynamic thermal properties of a multilayered wall using thermal impulse response (TIR) functions and the least square estimator based on data from in-situ (stochastic) experimental measurements. Even though the method seemed promising, the measurement duration was relatively high (12.5 days), and the results lacked of precision for the decrement factor and modulus of periodic thermal transmittance with a relative difference of about 30%.

Transient heating has been investigated in some research applications for determining the dynamic thermal properties of building walls. Robinson et al. [14] used a transient heating method with an imposed high temperature boundary condition to determine the dynamic thermal properties of an experimental wall by comparing the measured heat flux with the analytical solution. Chaffar et al. [15] used the same approach by applying a flat resistance heating surface against an experimental wall insulated from behind to direct the dissipated power towards the wall; the temperature response was recorded using infrared thermography. Soret et al. [16] also used a stainless steel 5 kW electric radiant heater to analyze transient heat flow for effective numerical fitting of thermophysical parameters and applied it for two conventional wall systems. Even though these methods give satisfactory results, they are not very suitable for in-situ applications because of the needed heavy and bulky instruments for imposing the required boundary conditions.

Deconinck et al. [17] compared five different characterization methods for determining the thermal resistance of building components using two semi-stationary methods (Average method, Storage effects) and three dynamic data analysis methods (Anderlind, ARX, GREY). They found that the dynamic methods not only converge much faster, but also provide accurate resistance estimates for summer data sets, while the semi-stationary methods did not lead to reliable results for summer measurements. This comprehensive study is very interesting but also lacks of estimating the dynamic thermal properties.

This paper offers three different numerical methods using direct measurements of temperature and heat flux allowing the non-destructive thermophysical characterization of building elements.

The determination of the thermophysical properties (the thermal conductivity λ and the heat capacity ρc_p) of walls relies on the measurement of the surface temperature of the wall and the heat flux on one of its surface. No specific imposed boundary conditions are thus required. The investigated methods are validated in experimental conditions using a heating box setup and a masonry brick wall. Random boundary conditions were imposed through a thermal heat box containing a thermo-regulated radiator. The reproducibility of the method was also validated through two other datasets: a random one with a different shape and different time step, and another one having a harmonic shape. The validity of the adopted methods is thus verified not only by comparing the optimal results of thermal conductivity and heat capacity obtained by the different methods for a same data set, but also by comparing the optimal results for two additional different data sets. After determining the equivalent thermal properties of the wall using the inverse problem, the direct method was used for comparing experimental measurements and numerical results for step temperature boundary conditions.

2 Experimental aspect

2.1 Experimental heating box

A 34 cm masonry brick wall [18-21] made of (6cm x 11cm x 22cm) solid bricks with mortar joints was tested through a heating box with a controlled atmosphere thanks to a radiator whose fluid is controlled by a thermostatic bath having a controlled temperature varying between 5°C and 60°C.

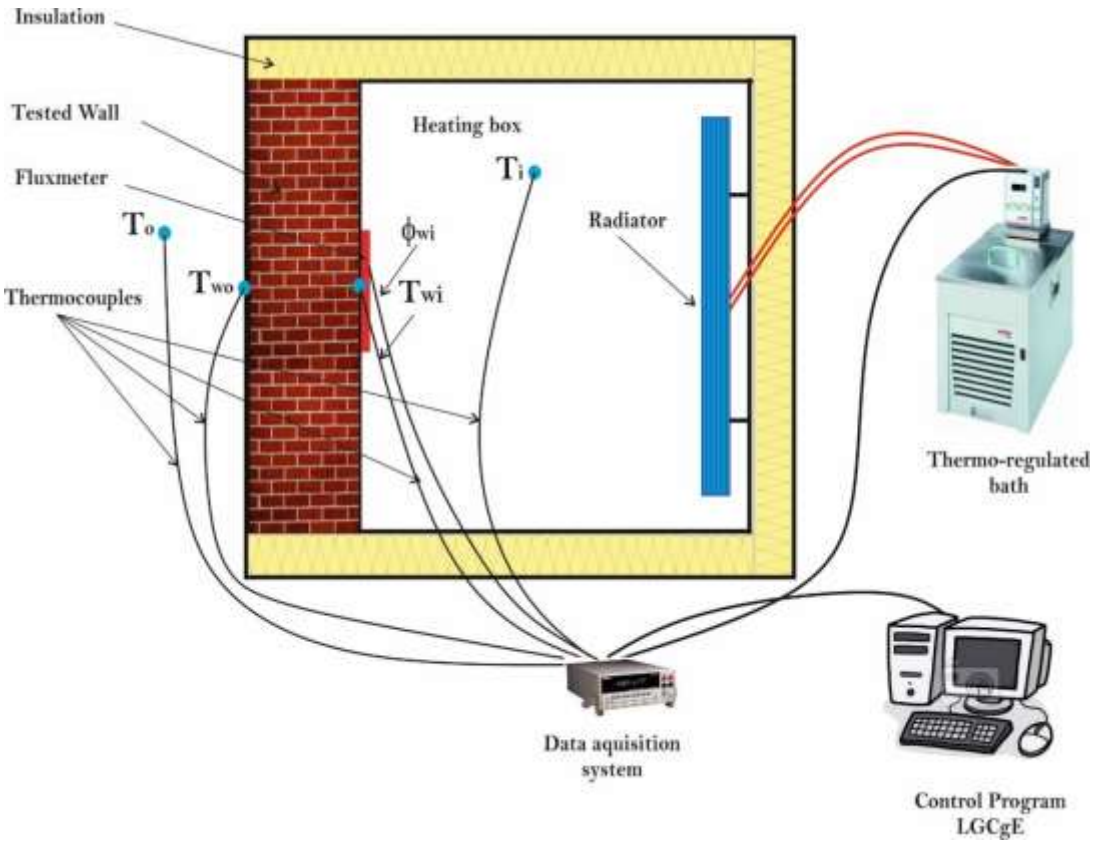

Figure 1- Vertical cross-section view of the experimental setup and boundary conditions

The box has a 91 cm width, a 93 height, and a 110 cm depth, and is insulated with 20 cm of Rockwool, which reduces the heat transfer to a unidirectional heat flow.

Fig. 1 represents a cross-section of the experimental device with its main components as well as the boundary conditions applied to the wall. Two thermocouples of type *T* give the inner and outer wall surface temperatures, and a heat fluxmeter measures the heat flow across the wall at the inner surface. The type of the used fluxmeter is ‘‘tangential gradient fluxmeter”, it has a thickness of about 0.5 mm, and a sensitivity of about 80 $\mu V.W^{-1}.m^{-2}$ for an active surface of 150 mm^2. All sensors were connected to a data logger (GL820) that records data with regular time steps. The masonry wall is considered homogeneous having the equivalent thermal properties λ and ρc_p.

2.2 Boundary conditions

The inside environment of the heating box represents the outdoor environment with stochastic temperature variations, while the laboratory atmosphere (outside the heating box) represents the indoor environment where the temperature varies slightly as shown in Fig. 2.

In real case scenarios, the solar radiation and wind convection constitute additional noise sources that must be considered:

- The natural convection caused by the wind will not affect the measurements since the inside and outside wall surface temperatures are measured and not the ambient temperatures. The convective heat transfer coefficients from the inside h_i and outside h_o are therefore not accounted.
- Solar radiation can be avoided by sheltering the wall from direct sunlight which excludes the direct impact of solar radiation on the external surface.

The radiator’s fluid temperature is defined by a set of values that were predefined and generated through a random function. The radiator’s fluid random temperature variation creates a random ambiance temperature T_i inside the heating box. T_{wi} and T_{wo} are respectively the inner and outer wall surface temperatures, and T_0 the temperature of the laboratory. These four temperature profiles, as well as the heat flux at the inner wall surface, were recorded for 4000 minutes (66.6 hours) with a 10 minutes’ time step and are shown in Fig. 2.

3 Numerical methods

3.1 Description of the numerical methods

The thermal properties were determined by using T_{wi} and T_{wo} as imposed temperature boundary conditions and by performing an identification between the measured and the numerical heat fluxes (φ_{i_exp} and φ_{i_num}). Two parameters (the thermal conductivity and the thermal capacity) were simultaneously optimized using three different optimization methods:

1.) The Heat Transfer Matrix analytical method using the heat transfer matrix, hereafter noted by HTM

2.) The Finite Element Method using COMSOL® multiphysics software, hereafter noted by FEM

3.) The Building Simulation Model method using TRNSYS® Type 56 coupled with Genopt® optimization program, hereafter noted by BSM

3.1.1 The Heat Transfer Matrix method (HTM)

According to EN ISO 13786, the transfer equation as a function of the Laplace variable "*p*" providing the relationship between the temperatures and heat fluxes on both sides of a homogeneous wall can be expressed as hyperbolic functions [10]:

$$\begin{bmatrix} T_{wo} \\ F_o \end{bmatrix} = \begin{bmatrix} ch\left(\sqrt{pRC}\right) & \sqrt{\frac{R}{pC}}sh\left(\sqrt{pRC}\right) \\ \sqrt{\frac{pC}{R}}sh\left(\sqrt{pRC}\right) & ch\left(\sqrt{pRC}\right) \end{bmatrix} \times \begin{bmatrix} T_{wi} \\ F_i \end{bmatrix} \quad (6)$$

R and *C* are the thermal resistance and the surface heat capacity of the considered layer; they are related to the optimized parameters through the following equations:

$$R = \frac{e}{\lambda} \quad (7)$$

$$C = \rho.C_p.e \quad (8)$$

The boundary temperatures $T_{wi}(t)$ and $T_{wo}(t)$ are decomposed into Fourier series and then the resulting heat flux from the constant and harmonic components of the random signal are evaluated separately. The method was detailed by the authors in previous studies [19, 20].

The optimization is performed using the Generalized Reduced Gradient algorithm (GRG2) mainly used in nonlinear optimization problems. The least squares method is used to minimize the sum of the differences between the measured and calculated heat fluxes [19] and thus reaching the optimized *R* and *C*.

3.1.2 The Finite Element Method (FEM)

COMSOL® Multiphysics simulation software was used for applying the Finite Element Method (FEM) for solving the heat transfer in solids model based on the following heat transfer equation:

$$\rho C_p \frac{\partial T}{\partial t} - \nabla \cdot (k \nabla T) = Q \quad (9)$$

Where *Q* is the heat source.

The thermophysical parameters of the wall (λ and ρc_p) were optimized using the Levenberg - Marquardt (LMA) algorithm. The LMA algorithm is used in many software applications to solve least-squares curve fitting problems. It was chosen for its speed of simulation and reliability [22].

3.1.3 The Building Simulation Model method (BSM)

In this method, the tested wall is considered as one of the walls of a simple building component, the remaining walls considered as adiabatic, and the optimization is done with respect to the heat loss through the wall. TRNSYS® software with its TRNBuild component is used for building thermal modeling. The TRNBUILD file contains the building description that will be used by the TYPE 56 component during TRNSYS® simulations.

The file containing the building description processed by the TRNBuild module can be generated by the user with any text editor or with the TRNBuild interactive program. The TYPE 56 building model is a non-geometric scale model with a zone air node, representing the thermal capacity of the air volume of the zone and the capabilities closely related to the air node.

The TRNSYS® heat transfer calculation model is based on the transfer function method that was introduced by Stephenson and Mitalas (1971) **[23]**.

Optimization was performed with GenOpt®, an optimization software that minimizes an objective function evaluated by an external simulation program (in this TRNSYS® study). It uses genetic algorithms to obtain an approximate solution to an optimization problem by using the notion of natural selection and applying it to a population of potential solutions to the given problem.

The boundary conditions are imposed on one of the walls in the TRNBuild interface of the TRNSYS® software, the other walls being adiabatic (extremely high thermal resistances).

The wall is subjected firstly to an imposed outdoor temperature boundary condition (T_0=T_{wi}), and secondly to an imposed indoor ambient temperature boundary condition (T_i=T_{wo}) with an internal convective exchange coefficient extremely high since it is not possible to impose Dirichlet boundary conditions (imposed temperature on the inner wall side) in TRNSYS®.

The three analyzed data are:

- The internal surface temperature of the wall "T_{SI}" (=T_{wo})

- The external surface temperature of the wall "T_{SO}" (=T_{wi})

- And the energy transferred to the outer surface "Q_{COMO}"

The latter represents the objective function that will be minimized by comparing it to the experimental flux measured at the inner surface of the wall (the side of the box) φ_i.

4 Results and discussion

4.1.1 Results for the three methods

The three numerical methods offer results that are clearly comparable with each other and with the experimental ones. This can be clearly observed by comparing the heat flux variation curves for the optimal values of λ and ρc_p (Fig. 2). The total simulation time is 66.6 hours (a little less than three days).

In order to define how well the measured and simulated heat fluxes are identical, the Nash-Sutcliffe efficiency coefficient (NSE) is calculated for the three different methods. It indicates how well the plot of measured versus simulated model data fits the 1:1 line. A value of *NSE*=1, corresponds to a perfect match of the model to the measurements; *NSE*=0, indicates that the model predictions are as accurate as the mean of the measurements data; and a negative value of *NSE*, indicates that the observed mean is a better predictor than the model [24].

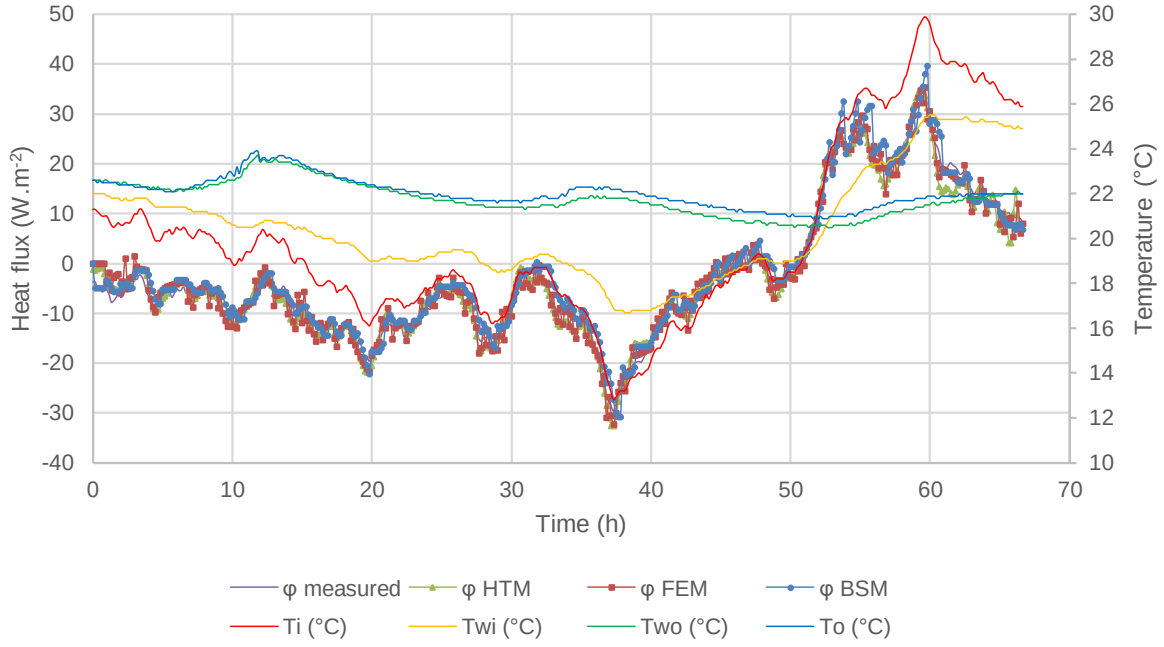

Figure 2- Comparison between experimental and numerical heat fluxes for the optimal solutions of the three methods

It is computed by:

$$NSE = 1 - \frac{\sum_{i=1}^{n}(OBS_i - SIM_i)^2}{\sum_{i=1}^{n}(OBS_i - \overline{OBS})^2} \quad (10)$$

Where "OBS_i" is the observed (or measured) value and "SIM_i" is the simulated value.

Fig. 3 shows that the *NSE* coefficient is close to 1 for the three different methods proving that the three methods provide comparably accurate results.

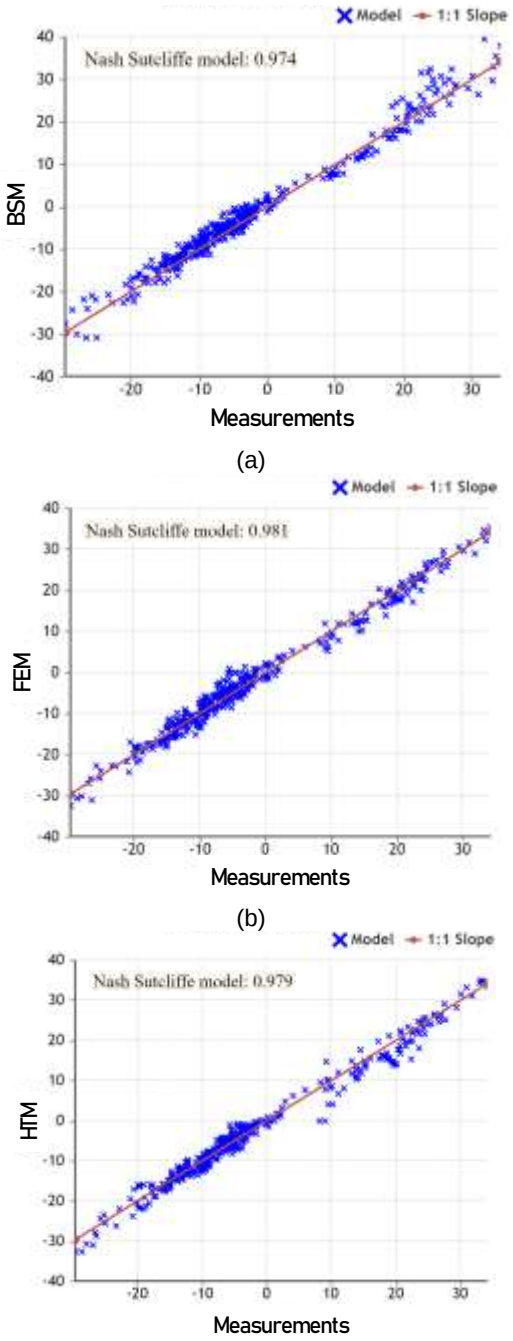

Figure 3- Nash Sutcliffe Efficiency coefficient (NSE) for the three different methods

The computation time for the analytical method is very low around 15s; however, for the numerical methods the durations are 3min 22s for COMSOL and 5min 55s for TRNSYS.

The comparison of the thermal conductivity results and thermal capacity in Table 2 shows the validity of the three methods and the admissible precision in the identification results with a maximum difference of 13% for λ and 9% for ρc_p.

Table 1- Comparison of thermal conductivity (a) and the heat capacity (b) results for the three proposed methods

	HTM	FEM	BSM
λ (W/m.K)	0.935	0.884	0.821
ρc_p (J/m^3.K)	853955	938880	922875

4.1.2 Comparison of the solutions' convergence

It is also interesting to investigate the speed of convergence of the three numerical methods while data logging with the aim of highlighting the method that can gives convergent results in the shortest time frame and with enough accuracy. In this work, convergence is defined as the data logging time from which the maximum difference between the optimized parameters using the three different methods is less than 5%. On the other hand, the convergence of the thermal conductivity (Fig. 4-a) and the heat capacity (Fig. 4-b) is not reached since the relative differences between the methods is 13% for λ and 9% for ρc_p. A longer dataset is thus needed for reaching more accurate results. This was expected since the measurement duration in the first dataset was longer (200 hours versus 66.6 hours for random dataset 1).

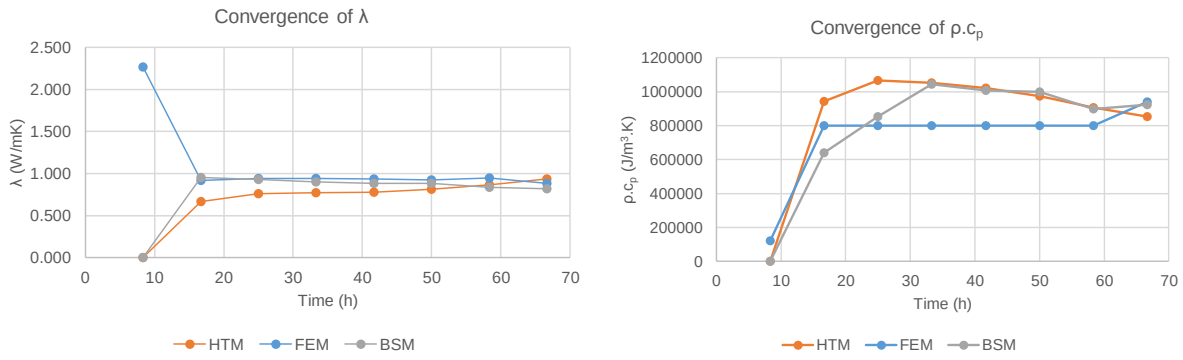

(a) (b)

Figure 4- Convergence of the thermal conductivity λ (a) and the heat capacity ρc_p (b) for the three numerical methods for the random dataset 1

4.2 Reproducibility of the methods for other datasets

Two additional datasets were analyzed to confirm the reproducibility of the method for the three signals and to check its accuracy.

The first additional investigated dataset presents a random temperature profile (random dataset 2), similar to the initial one with another profile shape and time step (30 minutes instead of 10 minutes) with the same number of recordings (400 values) and thus a total data logging duration of 200 hours as shown in Fig. 5.

The comparison between the experimental and numerical heat fluxes for random dataset 2 for the optimal solutions obtained by the three methods shows a good accuracy as shown in Fig. 6.

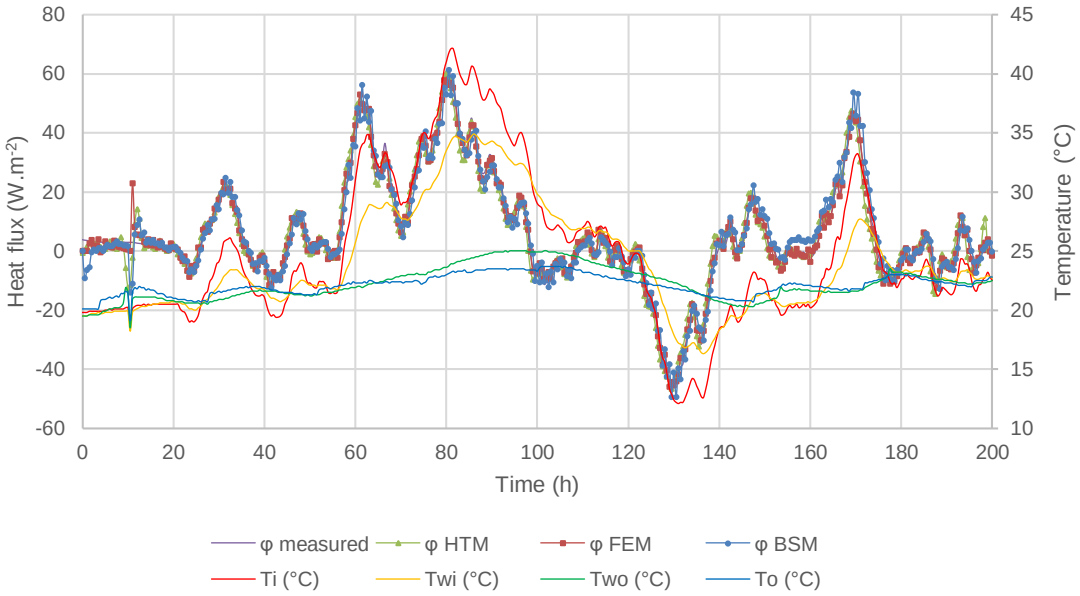

Figure 5- Comparison between experimental and numerical heat fluxes for the optimal solutions of the three methods for random dataset 2

On the other hand, Fig. 6 shows that the three methods need around 5 days (125h) for reaching accurate and convergent values for both λ and ρc_p for the three numerical methods. No method presents a remarkable advantage compared to the others which confirms the paramount importance of the duration of measurements as for the determination of the dynamic thermophysical properties of the walls. The convergence of the thermal conductivity (Fig. 6-a) and the heat capacity (Fig. 6-b) is more pronounced compared to the initial case (Fig. 4-a, and Fig. 4-b). Another interesting fact is that λ and ρc_p converge simultaneously for a same data logging duration (125h). The maximum deviation after 200h of data logging is 5% for λ and 3% for ρc_p.

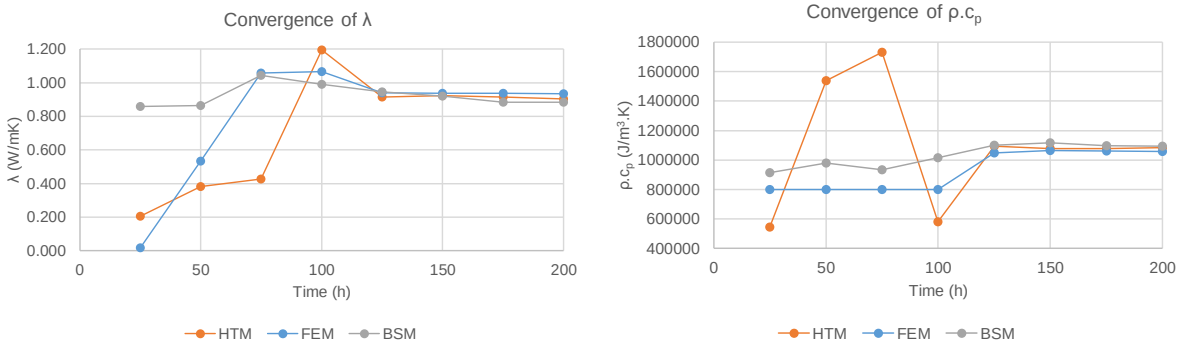

(a) (b)

Figure 6- Convergence of the thermal conductivity λ (a) and the heat capacity ρc_p (b) for the three numerical methods

The second additional case is a harmonic case also with a time step interval of 10 minutes and a total duration of 66.6 hours. The set temperature profile of the radiator in the experimental setup has a sinusoidal shape with a period of 24h, an average temperature of 40°C and amplitude of 20°C, this generates the ambiance and wall surface temperature profiles shown in Fig. 7.

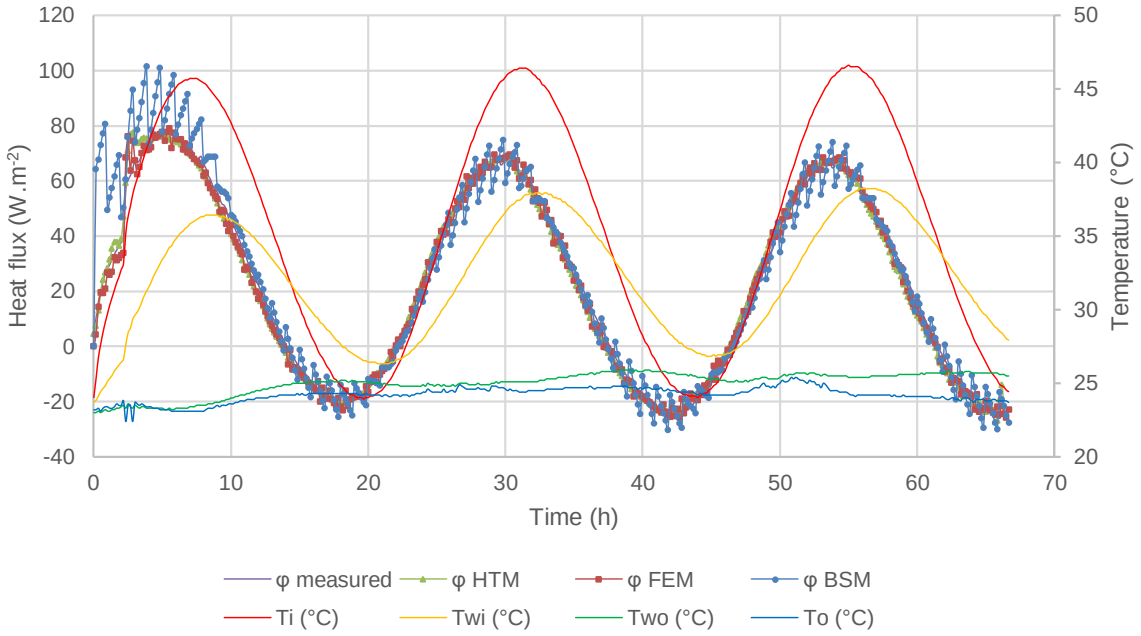

Figure 7- Comparison between experimental and numerical heat fluxes for the optimal solutions of the three methods for the harmonic dataset

The comparison between the experimental and numerical heat fluxes for the harmonic dataset for the optimal solutions obtained by the three methods also shows a good accuracy as shown in Fig. 7. The convergence of the thermal conductivity (Fig. 8-a) and the heat capacity (Fig. 8-b) is reached after 50 hours (~ 2 days) unlike the case of the initial random dataset that has the same time step and data logging durations. Therefore, the results favor the application of signals having a harmonic shape to be used as boundary condition for thermal characterization of walls in the laboratory or in situ. The maximum deviation after 66h of data logging is 2% for λ and 5% for ρc_p.

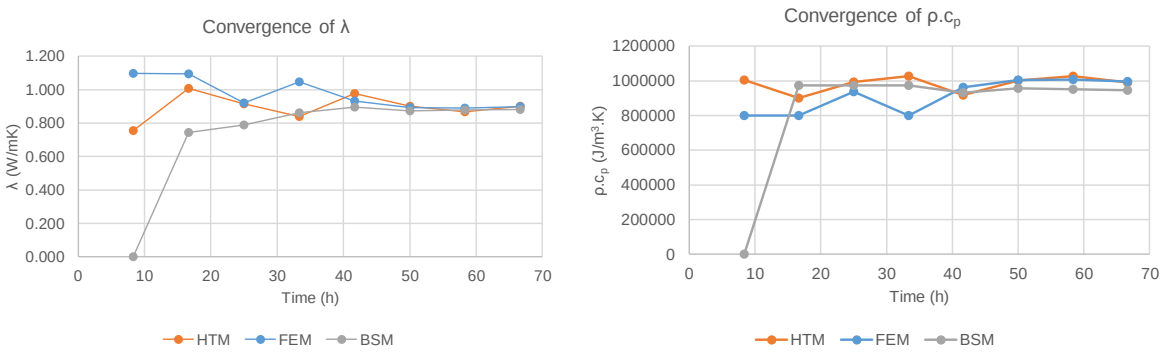

(a) (b)

Figure 8- Convergence of the thermal conductivity λ (a) and ρc_p (b) for the three numerical methods for the harmonic dataset

The comparison of the results in Table 3 shows that the three methods with the three case studies give accurate results for both the thermal conductivity and the heat capacity. The results show that the variability of the values obtained is related to two main factors: the boundary conditions and the method used.

The average thermal conductivity for the nine cases is 0.893W/m.K and the maximum deviation from this value is 8% while the average heat capacity for the nine cases is 987119J/m^3.K and the maximum deviation from this value is 13%.

Table 2- Comparison of the optimal results for the three methods and for the three case studies

	λ (W/m.K)			ρc_p (J/m^3.K)		
Dataset	HTM	FEM	BSM	HTM	FEM	BSM
Random 1	0.935	0.884	0.821	853955	938880	922875
Random 2	0.902	0.935	0.884	1084187	1058000	1095500
Harmonic	0.899	0.899	0.881	989490	994930	946250

4.3 1D direct numerical method in transient step boundary conditions

The transient step boundary conditions do not allow determining the dynamic thermal properties of walls in inverse heat transfer problem since the temperature variation intervals are very small. The experimental measurements of temperature and heat fluxes were used to validate the equivalent thermal properties of the wall in direct simulation method instead of adopting the inverse problem approach. The total time is 666h and the used time step is 1h. The equivalent thermal properties used for the wall are 0.9 W.m^{-1}.K^{-1} and 1000000 J.m^{-3}.K^{-1}.

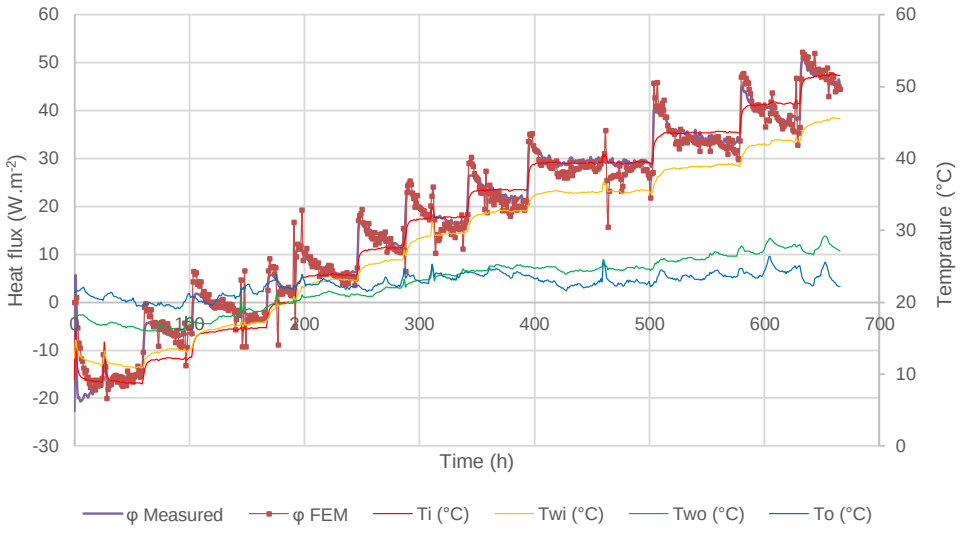

Figure 9- Comparison between experimental and numerical heat fluxes for the optimal thermal properties using transient step temperature boundary conditions

The heating box temperature variation is obtained by imposing constant set temperatures of 5°C; 10°C; 15°C; 20°C; 25°C; 30°C; 35°C; 40°C; 45°C; 50°C; 55°C and 60°C to the thermostatic bath of the radiator. The boundary conditions are shown in Fig. 9.

The results show that the numerical and experimental heat fluxes are very comparable except some values caused by some noises from the heating box temperature T_i and the ambient air temperature outside the heating box T_o. These results validate the accuracy of the thermal equivalent thermal properties used for the wall (0.9 $W.m^{-1}.K^{-1}$ and 1000000 $J.m^{-3}.K^{-1}$) and the different thermal characterization approaches used for this purpose. The *NSE* coefficient is 0.976 which confirms a perfect match between the numerical and experimental heat flux values for the optimized thermal properties λ and ρc_p.

5 Conclusion

This work highlights three different numerical methods allowing the thermal characterization of the existing walls through simple non-destructive tests based on the measurement of the temperatures of the walls on both sides as well as one of the heat fluxes (preferably the outside heat flux). The comparison of the three methods confirms their applicability and gives very similar values for both the thermal conductivity and the thermal capacity.

Furthermore, the study of the reproducibility of the results confirmed the accuracy of the three methods allowing a better identification of thermophysical parameters.

The obtained results were satisfactory for λ and for ρc_p for the three studied methods with deviations less than 5% between the results of the different methods for both λ and ρc_p when the data logging durations were long enough. The data logging duration for random conditions was found to be around five days while in harmonic boundary conditions two days were sufficient for the solution to converge. These three methods are thus applicable and could be used to determine the thermophysical properties of existing walls with a relatively simple instrumentation and moderate measurement duration. The recommended data logging duration was found to be beyond 125 hours. The adopted methodology can be used for any building envelope type and requires regular recordings to take place every 30 (or 60) minutes and an optimization calculation to be performed every 5 hours by performing an identification between the theoretical flux $\varphi_{num\text{-}wo}$ that can be computed using the inside and outside measured surface temperatures T_{wi} and T_{wo} and the experimental heat flux $\varphi_{exp\text{-}wo}$ in order to deduce the optimal values of λ and ρc_p. The data acquisition stops when 3 consecutive optimization values of λ and ρc_p converge. The accuracy of the optimized thermal parameters was also validated in direct heat transfer problem in transient step temperature boundary conditions.

References

[1] W. Natephra, N. Yabuki, T. Fukuda, “Optimizing the evaluation of building envelope design for thermal performance using a BIM-based overall thermal transfer value calculation”, *Building and Environment* 136 (2018) 128-145

DOI: 10.1016/j.buildenv.2018.03.032
[2] EN ISO 6946, Building Components and Building Elements – Thermal Resistance and Thermal Transmittance – Calculation Method, 2007.
[3] R. Bruno, P. Bevilacqua, G. Cuconati, N. Arcuri, “An innovative compact facility for the measurement of the thermal properties of building materials: first experimental results”, *Applied Thermal Engineering* 143 (2018) 947-954
DOI: 10.1016/j.applthermaleng.2018.06.023
[4] L. Evangelisti, C. Guattari, F. Asdrubali, “Comparison between heat-flow meter and Air-Surface Temperature Ratio techniques for assembled panels thermal characterization”, *Energy & Buildings* 203 (2019) 109441
DOI: 10.1016/j.enbuild.2019.109441
[5] C. Cornaro, F. Bucci, M. Pierro, M. E. Bonadonna, G. Siniscalco, “A new method for the thermal characterization of transparent and semi-transparent materials using outdoor measurements and dynamic simulation”, *Energy and Buildings* 104 (2015) 57–64
DOI: 10.1016/j.enbuild.2015.06.081
[6] EN ISO 9869-1, Thermal Insulation – Building Elements – In-Situ Measurement of Thermal Resistance and Thermal Transmittance. Part 1: Heat Flow Meter Method, 2014.
[7] A. Rasooli, L. Itard, “In-situ characterization of walls’ thermal resistance: An extension to the ISO 9869 standard method”, *Energy & Buildings* 179 (2018) 374–383
DOI: 10.1016/j.enbuild.2018.09.004
[8] J. Berger, H. Orlande, N. Mendes, S. Guernouti, “Bayesian inference for estimating thermal properties of a historic building wall”, *Building and Environment* 106 (2016) 327-339
DOI: 10.1016/j.buildenv.2016.06.037
[9] V. Gori, V. Marincioni, P. Biddulph, C. Elwell, “Inferring the thermal resistance and effective thermal massdistribution of a wall from in situ measurements to characterise heattransfer at both the interior and exterior surfaces”, *Energy and Buildings* 135 (2017) 398–409
DOI: 10.1016/j.enbuild.2016.10.043
[10] EN ISO 13786, Thermal Performance of Building Components – Dynamic Thermal Characteristics – Calculation Methods, 2008.
[11] Z. Petojević, R. Gospavić, G. Todorović, “Estimation of thermal impulse response of a multi-layer building wall through in-situ experimental measurements in a dynamic regime with applications”, *Applied Energy* 228 (2018) 468–486
DOI: 10.1016/j.apenergy.2018.06.083
[12] G. Baldinelli, F. Bianchi, A. Lechowska, J. Schnotale, “Dynamic thermal properties of building components: Hot box experimental assessment under different solicitations”, *Energy & Buildings* 168 (2018) 1–8
DOI: 10.1016/j.enbuild.2018.03.001
[13] R. Ricciu, A. Galatioto, L. Besalduch, S. Gana, A. Frattolillo, “Thermal properties of building walls: Indirect estimation using the inverse method with a harmonic approach”, *Energy & Buildings* 187 (2019) 257–268

DOI: 10.1016/j.enbuild.2019.01.035
[14] A. J. Robinson, F. J. Lesage, A. Reilly, G. Mc Granaghan, G. Byrne, R. O'Hegarty, O. Kinnane, "A new transient method for determining thermal properties of wall sections", *Energy and Buildings* 142 (2017) 139-146
DOI: 10.1016/j.enbuild.2017.02.029
[15] K. Chaffar, A. Chauchois, D. Defer, L. Zalewski, "Thermal characterization of homogeneous walls using inverse method", *Energy and Buildings* 78 (2014) 248-255
DOI: 10.1016/j.enbuild.2014.04.038
[16] G. M. Soreta, D. Lázarob, J. Carrascala, D. Alvearb, M. Aitchisonc, J. L. Toreroa, "Thermal characterization of building assemblies by means of transient data assimilation", *Energy and Buildings* 155 (2017) 128–142
DOI: 10.1016/j.enbuild.2017.08.073
[17] A. Deconinck, S. Roels, "Comparison of characterization methods determining the thermal resistance of building components from onsite measurements", *Energy and Buildings* 130 (2016) 309–320
DOI: 10.1016/j.enbuild.2016.08.061
[18] E. Sassine, Z. Younsi, Y. Cherif, A. Chauchois, E. Antczak, "Experimental determination of thermal properties of brick wall for existing construction in the north of France", *Journal of Building Engineering* 14 (2017) 15–23
DOI: 10.1016/j.jobe.2017.09.007
[19] E. Sassine, "A practical method for in-situ thermal characterization of walls", *Case Studies in Thermal Engineering* 8 (2016) 84–93
DOI: 10.1016/j.csite.2016.03.006
[20] E. Sassine, Z. Younsi, Y. Cherif, E. Antczak, "Thermal performance evaluation of a massive brick wall under real weather conditions via the Conduction Transfer function method", *Case Studies in Construction Materials* 7 (2017) 56–65
DOI: 10.1016/j.cscm.2017.04.003
[21] E. Sassine, Z. Younsi, Y. Cherif, E. Antczak, "Frequency domain regression method to predict thermal behavior of brick wall of existing buildings", *Applied Thermal Engineering* 114 (2017) 24–35
DOI: 10.1016/j.applthermaleng.2016.11.134
[22] E. Sassine, Y. Cherif, E. Antczak, "Parametric identification of thermophysical properties in masonry walls of buildings", *Journal of Building Engineering* 25 (2019)
DOI: 10.1016/j.jobe.2019.100801
[23] Stephenson, D. G., Mitalas, G. P., "Calculation of heat conduction transfer functions for multilayer slabs", *ASHRAE Trans.* 77 (1971) 117–126
[24] AgriMetSoft (2019). Online Calculators. Available on:
https://agrimetsoft.com/calculators/Nash%20Sutcliffe%20model%20Efficiency%20coefficient